<Research Report>Silicon carbide: a new superconductor in the diamond family

AUTHOR(S):

Kriener, Markus

CITATION:

Kriener, Markus. <Research Report>Silicon carbide: a new superconductor in the diamond family. 低温物質科学研究センター誌 : LTMセンター誌 2008, 12: 28-35

ISSUE DATE:

2008-06-01

URL:

https://doi.org/10.14989/153217

Silicon carbide: a new superconductor in the diamond family

M. Kriener
Department of Physics, Kyoto University

1. Introduction

Diamond and silicon are wide-gapped semiconductors / insulators which exhibit indirect energy gaps of about 5.5 eV (diamond) and 1.1 eV (silicon). They are well-known for their outstanding physical properties and technical applications, e.g. the excellent heat conductivity of diamond, its withstanding of high electric fields, or the numberless applications of silicon in semiconductor technologies.

It is well-known, too, that the physical properties of these and other semiconductors can be influenced by charge-carrier doping either by donator or acceptor atoms which changes their resistivity many orders of magnitude leading to intriguing properties. Small doping concentrations are widely used in the application of semiconductors. At higher doping levels the systems undergo an insulator-to-metal transition above a certain critical doping level, i.e. charge-carrier concentration, and further doping might even lead to superconductivity.

From the theoretical and experimental point of view superconductivity in doped semiconductors is an outstanding issue. The prediction of superconductivity in Ge and GeSi and the suggestion that other semiconductor-based compounds may exhibit superconductivity at very low temperatures were already given by Cohen in 1964 [1].

Indeed, some examples have been reported so far, e.g. self-doped Ge_xTe [2], Sn_xTe [3], doped $SrTiO_3$ [4], or more recently doped silicon clathrates. [5 – 7] The superconductivity of the latter materials is the first example of compounds exhibiting superconductivity and realizing a covalent tetrahedral sp^3 network with bond lengths similar to those in diamond.

However, before 2004 (C:B) [8] and 2006 (Si:B) [9] superconductivity was never reported for diamond and cubic silicon in the diamond structure although there are several studies available concerning hole-doped induced metallicity in silicon and carbon using boron, nitrogen, or phosphorus, e.g. Refs. [10], [11] and references therein. Therefore, it was an important progress to find superconductivity in these compounds upon boron doping, which attracted a lot of interest and stimulated many theoretical and experimental studies in the last four years [12 – 25]. Boron has one electron less than carbon and silicon and hence acts as an acceptor leading to hole doping. Both compounds are type-II superconductors with T_c values of 11.4 K (C:B) and 0.35 K (Si:B). The upper critical fields are $H_{c2} \approx 8.7$ T and 0.4T, respectively [9,19].

In order to explain the superconductivity in diamond theoretical studies point towards two different scenarios: (i) it is the result of a simple electron-phonon interaction [13,14,16,18] and (ii) it is caused by a resonating valence-bond mechanism [12,26,27]. The former model is based on a conventional

weak-coupling electron-phonon mechanism where the charge carriers are introduced into intrinsic diamond bands leading to a three-dimensional analog of the two-dimensional superconductor MgB_2. The superconductivity is attributed to holes located at the top of the zone-centered σ-bonding valence bands which couple strongly to optical bond-stretching phonon modes [14,16]. The latter model attributes the superconductivity to holes in the impurity bands rather than in the intrinsic diamond bands [12]. With the premise that the doping level in superconducting diamond is close to the Mott limit the randomly distributed boron atoms, i.e. their random Coulomb potential, may lift the degeneracy of the boron acceptor states leading to a narrow half-filled band from which superconductivity develops.

However, experimental studies seem to support the former explanation and rule out the latter suggestion [28,29], although a complete understanding of the superconducting phase is not yet obtained [27,30]. Recently, a theoretical study suggested the possibility to achieve superconducting transition temperatures of the order of 100 K in C:B due to the exceptionally high Debye temperature of diamond and under the precondition that the doped boron atoms are ordered [24].

In Ref. [31], we reported the discovery of superconductivity in a closely related system originating from a well-known and widely used semiconductor, namely boron-doped SiC, the stoichiometric "mixture" of the two afore discussed "parent" materials. SiC is more and more used for high-temperature, high-power, and high-frequency applications due to its high thermal conductivity, the existence of large band gaps, strong covalent bondings, chemical inertness, or its high withstand of radiation. Another hallmark of this system is the huge number (about 200) of crystal modifications with cubic ("C"), hexagonal ("H"), or rombohedral ("R") symmetry of the unit cell [32]. They are usually referred to as *m*C-SiC, *m*H-SiC, and *m*R-SiC, respectively.

The variable *m* gives the number of Si – C bilayers consisting of a C and a Si layer stacking in the unit cell. However, most of the available studies refer to the following three polytypes: cubic 3C- (zincblende structure, space group F-43m; "ordered" diamond) and hexagonal 2H-, 4H-, and 6H-SiC (wurtzite, moissanite-4H, and -6H structure, all space group $P6_3mc$). The 2H-modification is the only "pure" hexagonal modification, all other *m*H-SiC polytypes consist of hexagonal and cubic elements. The cubic 3C-modification is also labeled as *β*-SiC whereas the hexagonal polytypes are generally denoted as *α*-SiC. Fig. 1 gives a sketch of (a) the diamond-related modification 3C-SiC and (b) the hexagonal 6H-SiC. The C – Si bilayers are emphasized. In 3C-SiC both elements form face-centered cubic sublattices which are shifted by (1/4, 1/4, 1/4) with respect to each other. Along the <111> direction the bilayer stacking of the diamond modification is ABC – ..., for the polytypes 2H-, 4H-,

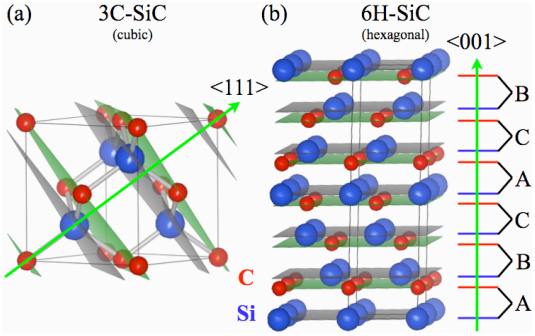

Figure 1: (a) Unit cell of diamond-related cubic 3C–SiC. The three bilayers consisting of C and Si layers are emphasized. The stacking sequence is ABC – ... The green arrow denotes the <111> direction whereas the gray rods refer to the tetrahedral bond alignment of diamond. (b) Four unit cells of hexagonal 6H–SiC. The six bilayers of the stacking sequence ABCACB – ... are emphasized. The green arrow denotes the <001> direction. For both drawings the software *Vesta* was used [33].

and 6H-SiC it is along the <001> direction ABAB – ..., ABAC – ..., and ABCACB – ...

Depending on the crystal modification, pure SiC exhibits an indirect energy gap between ~2 eV (3C-SiC) and ~3.3 eV (2H-SiC). Slightly doped SiC with donors and acceptors was intensely studied for nitrogen, phosphorus, boron, aluminum, etc. by ion-implantation or thermo-diffusion doping. Compared with other dopants, boron was found to have a much faster diffusion rate in SiC. Diffusion processes mediated by the silicon interstitials and by carbon vacancies have been proposed to explain such fast diffusion rates [34 – 37]. Under silicon-rich conditions the carbon-site substitution is dominating [38]. Among other dopants, the insulator-to-metal transition was observed recently in nitrogen-doped 4H-SiC at carrier concentrations above $10^{19}cm^{-3}$ [39].

Here we report resistivity and AC susceptibility of SiC:B. We discuss the $H - T$ phase diagram derived from AC susceptibility measurements and give a brief comparison of C:B and SiC:B focussing on the question, why SiC:B is a type-I superconductor whereas the „parent" compound C:B is of type-II.

2. Experiment

Samples were prepared from submicron β-SiC powder (99%, WAKO, with a mean particle size of 0.27 μm), silicon (99.99%), and amorphous boron (99%) by substitutional reaction sintering. The powders were mixed in certain proportions (typically SiC/B/Si with 4:1:1 in molar ratio), ground thoroughly, and pressed into cylindrical pellets. They were then placed in an alumina boat (or tantalum box) and sintered in a pre-evacuated tube furnace at 1620 ^{o}C for 12 hours (with heating and cooling rates of 100 ^{o}C per hour) in a flowing mixed argon/hydrogen gas atmosphere (60/60 ml per minute). The as-prepared samples were cut into slices and the surface was removed for transport measurements to better characterize the bulk properties. The crystal grain morphology was examined by a field-emission scanning electron microscopy (FESEM, JEOL JSM6301F). An electron-probe microanalyzer with wavelength dispersive spectrometers (EPMA-WDS, JEOL JXA8200S) was employed for a quantitative elemental composition analysis. Powder X-Ray diffraction (XRD) and Rietveld method were used for phase identification and lattice parameter refinement [40]. The electrical resistivity was measured by a conventional four-probe technique, the Hall coefficient by a five-probe AC technique with scanning fields from -7 to 7 Tesla using a commercial system (Quantum Design, PPMS). AC susceptibility measurements were performed using a mutual-inductance method in a commercial ^{3}He refrigerator (Oxford Instruments, Heliox) inserted into a standard superconducting magnet.

3. Analysis

The sintered samples have a black ceramic-like appearance but are not of single phase. Phase transformation from 3C-SiC to 6H-SiC was reported to occur above 1700^{o}C [41]. However, due to the well-known thermodynamic size-effect [42], i.e. small particles exhibit a reduced activation energy for melting, grain growth, or phase transformation, the transformation temperature may be lower. We identified three phase fractions by XRD pictures: 3C-SiC, 6H-SiC, and Si. No boron peaks were detected. The volume fraction of the 6H phase can be estimated from the XRD peak intensity ratios based on the empirical formula of Ruska *et al*. [43]. Typically, 10-30% 3C phase is converted into 6H-SiC upon sintering. We expect that the presence of liquid silicon facilitates the boron diffusion due to the much faster mass

transport compared to solid sintering, and enhances the boron-substitution efficiency. This also enhances the carbon site substitution by silicon. The lattice parameter for the silicon peaks did not change during the sinter process, indicating that no boron was doped into silicon.

For the main phase 3C-SiC, the refined lattice parameter *a* increased after sintering, but merely by less than 0.1% from 4.3575(3) Å to 4.3618(4) Å. The XRD peaks related to the 6H phase did not change within the experimental resolution. Since the atomic sizes of boron and carbon are comparable, but are much smaller than the atomic size of silicon, the minute change of the lattice parameters suggests that boron substitutes at the carbon site in these samples. The crystal grain size grew more than an order of magnitude after sintering, as could be shown by FESEM images (not shown). We expect the boron substitution to be enhanced with a slow growth of crystal grains, and indeed by the present synthetic method, the samples had much higher boron doping levels compared with previous reports [34 – 37]. EPMA analysis with area-scans (within 50×50 μm^2) at various positions occasionally detected less than 0.05 at.% Fe besides of Si, C, and B for all samples without other impurity elements. The point analysis within 1×1 μm^2 on crystal grains revealed less than 6 at.% boron, but this may include unreacted boron not incorporated in the SiC structure, or unactivated boron doped into the interstitial site of SiC without providing charge carriers. Room-temperature Hall-coefficient measurements were carried out for two samples, referred to as SiC-1 and SiC-2 in the following. The starting SiC/B/Si molar ratios were 4:1.15:1 for SiC-1 and 4:0.9:1 for SiC-2. The deduced effective hole carrier concentrations for SiC-1 and SiC-2 were 1.91×10^{21} cm^{-3} and 1.06×10^{21} cm^{-3}, corresponding to a boron substitution of 3.9 and 2.2 at.% in the carbon site.

4. Resistivity and AC susceptibility

In Fig. 2 the temperature dependence of the electrical resistivity for SiC-1 and SiC-2 is shown. Reflecting the high level of doping both samples become metallic. However, SiC-1 exhibits a much smaller resistivity and almost linear temperature dependence at high temperatures due to a higher boron-doping concentration. The slope $d\rho/dT$ is always positive for SiC-1, whereas a small negative $d\rho/dT$ is observed below 20 K for SiC-2, suggesting a weak tendency of localization of the carriers or a contribution from non-metallic grain boundary resistance. The residual resistance ratio *RRR* (ρ_{300K}/ρ_{5K}) is 10 and 5 for SiC-1 and SiC-2. The inset of Fig. 2 shows an expanded view of the low-temperature data. Below 1.4 K (SiC-1) and 1.35 K (SiC-2), the resistivity drop indicates a clear superconducting transition. We note that despite the large difference in the residual resistivity, T_c is nearly the same and the transition width is less than 0.15 K for both samples.

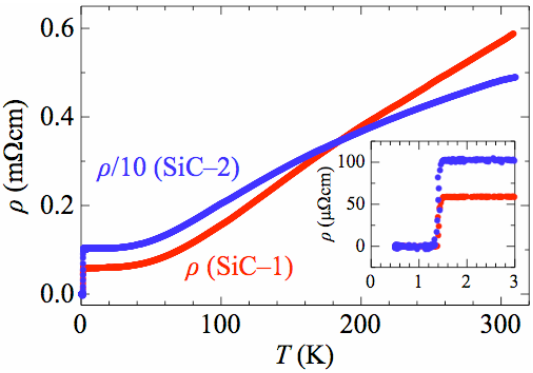

Figure 2: (a) Temperature dependence of the electrical resistivity for SiC-1 and SiC-2. For comparison, the resistivity of SiC-2 was divided by 10. The inset shows the normalized low-temperature resistivity R/R_{4K} around the superconducting transition temperature for both samples.

For SiC-1 temperature-dependent AC susceptibility was measured with a small AC field of H_{AC} = 0.01 Oe-rms at a frequency of 3011 Hz in zero and several finite DC magnetic fields H_{DC} parallel to H_{AC}. The measurements were performed upon cooling and

warming at constant H_{DC} as well as upon sweeping H_{DC} up and down at constant temperature. The temperature dependence of the in-field susceptibility data was taken as follows: The external DC magnetic field was set above T_c. Then the temperature was reduced down to ca. 300 mK ("field-cooling (FC) run") and subsequently increased above T_c ("warming after FC run"). In Fig. 3 the real part χ' and the imaginary part χ'' of the AC susceptibility for H_{DC} = 0, 20, 40, 60 Oe are shown. In zero DC magnetic fields only one transition is found with a T_c of ~1.45 K, in good agreement with the resistivity. In finite fields a large supercooling effect was observed. To exclude the possibility of a poor thermal coupling between sample and thermometer, we subsequently repeated measurements at different temperature sweep rates (not shown). We obtained the same curves independent of the chosen sweep rate, guaranteeing that the observed supercooling behavior is an intrinsic property of the sample and that the superconducting transition is a first order phase transition in finite fields. We note that the hysteresis was also observed in the field-dependence of the AC susceptibility. Above about 110 Oe we didn't find any sign of superconductivity. The observations of (i) the in-field hysteresis, (ii) the absence of a hysteresis in zero field, and (iii) the very small value of the critical field give strong evidence for type-I superconductivity. In this case, the observed critical field on warming corresponds to the thermodynamic critical field $H_c(0)$, as discussed later.

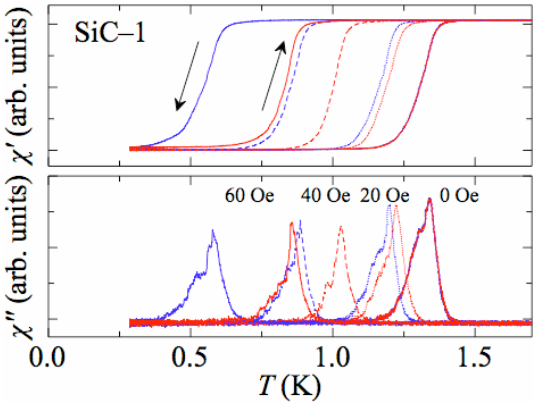

Figure 3: Temperature dependence of AC magnetic susceptibility for SiC-1 measured in different DC magnetic fields. The upper panel shows the real part $\chi'(T)$ and the lower panel the immaginary part $\chi''(T)$. The DC fields were applied above T_c. The data was taken upon field-cooling and subsequent warming as indicated by the arrows.

The AC susceptibility signals are very robust. The value of the shielding fraction in the real part χ' is almost field-independent. The imaginary part χ'' features additional shoulder peaks at the low-temperature side, which is probably due to an inclusion of superconducting grains with slightly lower T_c. Single phase samples or single crystals are desirable for future investigations.

5. *H – T* phase diagram and discussion

The $H - T$ phase diagram deduced from the AC magnetic susceptibility is shown in Fig. 4. We determined $T_c(H_{DC})$ from the onset of superconductivity in the χ' curves for both the field-cooling run (normal-to-superconducting transition) and the subsequent warming run (superconducting-to-normal transition). Applying the conventional formula $H_c(T) = H_c(0)[1-(T/T_c(0))^{\alpha}]$, we obtained a good fitting with $\alpha \approx 1.7$ of the warming-run data. As discussed in Ref. [31], we identify this as the line of the thermodynamic critical field $H_c(T)$ with $H_c(0) = (115\pm5)$ Oe. The same procedure applied to the cooling-run data yields $\alpha \approx 1.5$. We identify this transition as the upper limit of the intrinsic supercooling limit. The corresponding transition field is denoted as H_{sc} (the subscript "sc" stands for "supercooling") with an estimated $H_{sc}(0) = (80\pm5)$ Oe.

The question arises why the superconductivity in SiC:B is of type I rather than of type II like in C:B [8] and Si:B [9]. First, the difference is reflected in the critical field strength, which is of the order of 100 Oe

for SiC:B in contrast to several Tesla for C:B and half a Tesla for Si:B. Together with the experimental finding of an in-field first-order superconducting phase transition in SiC:B and the low value of H_c, this points towards a type-I nature. Second, Sidorov *et al.* [44] report in their specific-heat study on C:B $\xi_0 \approx 9$ nm (deduced from H_{c2}) and $\lambda \approx 163$ nm (from n and γ). This leads to $\kappa_{GL} \approx 18$ for C:B, which places this compound into the type-II region. From a specific-heat study using the sample SiC-1 we find $\kappa_{GL} \approx 0.36 < 1 / \sqrt{2}$, i.e. the "border line" between type-I and type-II superconductors, further supporting our conclusion that SiC:B is of type I [45]. Unfortunately, for Si:B there is no specific-heat study available yet.

As far as we know, at the current state of research, one may only speculate about the physical reasons behind it. One possibility could be a much different Fermi velocity v_F in the case of SiC:B due to a possible different shape of the Fermi surface. To clarify this, further experimental and theoretical work is necessary.

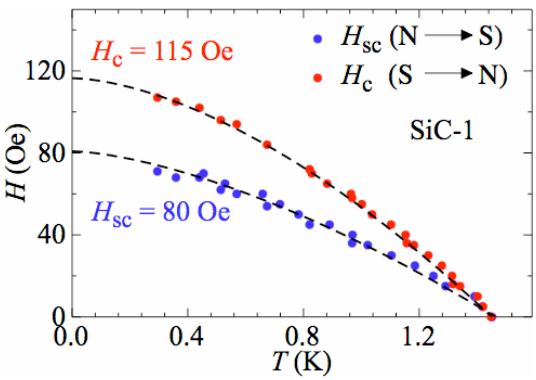

Figure 4: *H–T* phase diagram for SiC-1, determined from the onset of superconductivity in $\chi'(T)$. The lower (upper) line corresponds to the cooling (warming) runs. The supercooling limiting field $H_{sc}(T)$ corresponds to a transition from the *normal to superconducting states*, whereas the thermodynamic critical field $H_c(T)$ denotes the transition from the *superconducting to normal states*. The dashed lines are fits to the data, see text for details.

In conclusion, we discovered bulk superconductivity in boron-doped SiC based on the diamond structure and prepared by a substitutional sintering method. The zero-field value of T_c is about 1.4 K and the thermodynamic critical field $H_c(0)$ was estimated as about 115 Oe. Moreover we found an in-field hysteresis between subsequent cooling and warming runs of the temperature-dependent AC susceptibility associated with a strong supercooling effect. This findings and a small value of the Ginzburg-Landau parameter κ give strong evidence for type-I superconductivity.

This work was done in collaboration with Y. Maeno, Kyoto University and the group of Prof. J. Akimitsu, Department of Physics and Mathematics, Aoyama-Gakuin University, Sagamihara, Kanagawa 229-8558, Japan: J. Kato, T. Muranaka, and Z.-A. Ren, who made the samples. This work was supported by the 21st century COE programs, "High-Tech Research Center" Project for Private Universities: matching fund subsidy, as well as "Diversity and Universality of Physics" from the Ministry of Education, Culture, Sports, Science and Technology (MEXT), and a Grand-in-Aid for Scientific Research on Priority Area from MEXT.

Literature

[1] M. L. Cohen, Rev. Mod. Phys. **36**, 240 (1964).

[2] R. A. Hein, J. W. Gibson, R. Mazelsky, R. C. Miller, & J. K. Hulm, Phys. Rev. Lett. **12**, 320 (1964).

[3] R. Hein and P. Meijer, Phys. Rev. **179**, 497 (1969).

[4] J. F. Schooley, W. R. Hosler, E. Ambler, and J. H. Becker, Phys. Rev. Lett. **14**, 305 (1965).

[5] H. Kawaji, H. Horie, S. Yamanaka, and M. Ishikawa, Phys. Rev. Lett. **74**, 1427 (1995).

[6] F. Grosche, H. Yuan, W. Carrillo-Cabrera, S. Paschen, C. Langhammer, F. Kromer, G. Sparn, M. Baenitz, Y. Grin, and F. Steglich, Phys. Rev. Lett. **87**, 247003 (2001).

[7] D. Connétable, V. Timoshevskii, B. Masenelli, J. Beille, J. Marcus, B. Barbara, A. Saitta, G.-M. Rignanese, P. Mélinon, S. Yamanaka, et al., Phys. Rev. Lett. **91**, 247001 (2003).

[8] E. A. Ekimov, V. A. Sidorov, E. D. Bauer, N. N. Mel'nik, N. J. Curro, J. D. Thompson & S. M. Stishov, Nature **428**, 542 (2004).

[9] E. Bustarret, C. Marcenat, P. Achatz, J. Kačmarčik, F. Lévy, A. Huxley, L. Ortéga, E. Bourgeois, X. Blase, D. Débarre, and J. Boulmer, Nature **444**, 465 (2006).

[10] P. Dai, Y. Zhang, and M. Sarachik, Phys. Rev. Lett. **66**, 1914 (1991).

[11] E. Bustarret, E. Gheeraert, and K. Watanabe, phys. stat. sol. (a) **199**, 9 (2003).

[12] G. Baskaran, condmat/0404286 (2004).

[13] X. Blase, C. Adessi, and D. Connétable, Phys. Rev. Lett. **93**, 237004 (2004).

[14] L. Boeri, J. Kortus, and O. Andersen, Phys. Rev. Lett. **93**, 237002 (2004).

[15] E. Bustarret, J. Kačmarčik, C. Marcenat, E. Gheeraert, C. Cytermann, J. Marcus, and T. Klein, Phys. Rev. Lett. **93**, 237005 (2004).

[16] K.-W. Lee and W. Pickett, Phys. Rev. Lett. **93**, 237003 (2004).

[17] Y. Takano, M. Nagao, I. Sakaguchi, M. Tachiki, T. Hatano, K. Kobayashi, H. Umezawa, and H. Kawarada, Appl. Phys. Lett. **85**, 2851 (2004).

[18] H. Xiang, Z. Li, J. Yang, J. Hou, and Q. Zhu, Phys. Rev. B **70**, 212504 (2004).

[19] H. Umezawa, T. Takenouchi, Y. Takano, K. Kobayashi, M. Nagao, I. Sakaguchi, M. Tachiki, T. Hatano, G. Zhong, M. Tachiki, and H. Kawarada, condmat/0503303 (2005).

[20] T. Yokoya, T. Nakamura, T. Matsushita, T. Muro, Y. Takano, M. Nagao, T. Takenouchi, H. Kawarada, and T. Oguchi, Nature **438**, 647 (2005).

[21] B. Sacépé, C. Chapelier, C. Marcenat, J. Kačmarčik, T. Klein, M. Bernard, and E. Bustarret, Phys. Rev. Lett. **96**, 097006 (2006).

[22] D. Wu, Y. Ma, Z. Wang, Q. Luo, C. Gu, N. Wang, C. Li, X. Lu, and Z. Jin, Phys. Rev. B **73**, 012501 (2006).

[23] E. Bourgeois and X. Blase, Appl. Phys. Lett. **90**, 142511 (2007).

[24] T. Shirakawa, S. Horiuchi, Y. Ohta, and H. Fukuyama, J. Phys. Soc. Japan **76**, 014711 (2007).

[25] Y. Takano, T. Takenouchi, S. Ishii, S. Ueda, T. Okutsu, I. Sakaguchi, H. Umezawa, H. Kawarada, and M. Tachiki, Diamond Rel. Mat. **16**, 911 (2007).

[26] G. Baskaran, Phys. Rev. Lett. **90**, 197007 (2003).

[27] G. Baskaran, Sci. Technol. Adv. Mat. **7**, S49 (2006).

[28] J. Kačmarčik, C. Marcenat, C. Cytermann, A. F. da Silva, L. Ortega, F. Gustafsson, J. Marcus, T. Klein, E. Gheeraert, and E. Bustarret, phys. stat. sol. (a) **202**, 2160 (2005).

[29] B. Sacépé, C. Chapelier, C. Marcenat, J. Kačmarčik, T. Klein, F. Omnès, and E. Bustarret, phys. stat. sol. (a) 203, 3315 (2006).
[30] J. Nakamura, T. Oguchi, N. Yamada, K. Kuroki, K. Okada, Y. Takano, M. Nagao, I. Sakaguchi, H. Kawarada, R. Perera, and D. L. Ederer, condmat/0410144 (2004).
[31] Z. Ren, J. Kato, T. Muranaka, J. Akimitsu, M. Kriener, and Y. Maeno, J. Phys. Soc. Japan **76**, 103710 (2007).
[32] J. Casady and R. Johnson, Sol. State Elec. **39**, 1409 (1996).
[33] K. Momma and F. Izumi, Commission on Crystallogr. Comput., IUCr Newslett. 7, 106 (2006).
[34] H. Bracht, N. Stolwijk, M. Laube, and G. Pensl, Appl. Phys. Lett. **77**, 3188 (2000).
[35] R. Rurali, P. Godignon, J. Rebollo, P. Ordejón, and E. Hernández, Appl. Phys. Lett. **81**, 2989 (2002).
[36] Y. Gao, S. Soloviev, and T. Sudarshan, Appl. Phys. Lett. **83**, 905 (2003).
[37] F. Gao, W. Weber, M. Posselt, and V. Belko, Phys. Rev. B **69**, 245205 (2004).
[38] M. Bockstedte, A. Mattausch, and O. Pankratov, Phys. Rev. B **70**, 115203 (2004).
[39] A. da Silva, J. Pernot, S. Contreras, B. Sernelius, C. Persson, and J. Camassel, Phys. Rev. B **74**, 245201 (2006).
[40] F. Izumi and T. Ikeda, Mater. Sci. Forum, **321-324**, 198 (2000).
[41] P. Krishna and R. C. Marshall, J. Cryst. Growth **9**, 319 (1971).
[42] Ph. Buffat and J-P. Borel, Phys. Rev. A **13**, 2287 (1976).
[43] J. Ruska, L. J. Gauckler, J. Lorenz, H. U. and Rexer, J. Mater. Sci., **14**, 2013 (1979).
[44] V. A. Sidorov, E. A. Ekimov, S. M. Stishov, E. D. Bauer, and J. D. Thompson. Phys. Rev. B **71**, 060502(R) (2005).
[45] M. Kriener, Y. Maeno, T. Oguchi, Z. A. Ren, J. Kato, T. Muranaka, and J. Akimitsu. submitted to Phys. Rev. B (2008).

Curriculum Vitae

1994 – 2001	studies of mathematics and physics, University of Cologne, Germany (ケルン，ドイツ)
02 / 2001	diploma in physics
07 / 2005	PhD in physics University of Cologne, Germany
08 / 2005 – 01 /2006	postdoc, University of Cologne, Germany
since 02 / 2006	postdoc, Quantum Materials Lab, Kyoto University